

This is the accepted manuscript made available via CHORUS. The article has been published as:

Absolute Instability near the Band Edge of Traveling-Wave Amplifiers

D. M. H. Hung, I. M. Rittersdorf, P. Zhang, D. Chernin, Y. Y. Lau, T. M. Antonsen, Jr., J. W. Luginsland, D. H. Simon, and R. M. Gilgenbach

Phys. Rev. Lett. **115**, 124801 — Published 16 September 2015

DOI: [10.1103/PhysRevLett.115.124801](https://doi.org/10.1103/PhysRevLett.115.124801)

August 25, 2015

Absolute instability near the band edge of traveling wave amplifiers

D. M. H. Hung¹, I. M. Rittersdorf^{1,2}, P. Zhang¹, D. Chernin^{1,3}, Y. Y. Lau^{1,*}, T. M. Antonsen⁴, Jr.,
J. W. Luginsland⁵, D. H. Simon¹, and R. M. Gilgenbach¹

¹Department of Nuclear Engineering and Radiological Sciences, University of Michigan, Ann Arbor, MI 48109, USA

²Present address: Naval Research Laboratory, Washington, DC 20375, USA

³Leidos Corporation, Reston, VA 20190, USA

⁴University of Maryland, College Park, MD 20742, USA

⁵Air Force Office of Scientific Research, Arlington, VA 22203, USA

ABSTRACT

Applying the Briggs-Bers ‘pole-pinch’ criterion to the exact transcendental dispersion relation of a dielectric traveling wave tube (TWT), we find that there is no absolute instability regardless of the beam current. We extend this analysis to the circuit band edges of a linear beam TWT by approximating the circuit mode as a hyperbola in the frequency-wavenumber (ω - k) plane and consider the weak coupling limit. For an operating mode whose group velocity is in the same direction as the beam mode, we find that the lower band-edge is not subjected to absolute instability. At the upper band-edge, we find a threshold beam current beyond which absolute instability is excited. The non-existence of absolute instability in a linear beam TWT and the existence in a gyrotron-TWT, both at the lower band edge, is contrasted. The general study given here is applicable to some contemporary TWT’s such as metamaterial-based and advanced Smith-Purcell TWT’s.

*Corresponding author: yylau@umich.edu

Unwanted oscillations pose a major threat to the operation of high power amplifiers. In a traveling wave tube (TWT) amplifier, when the electron beam current is too high, the amplifier oscillates. Three types of oscillations may occur: (a) regenerative type [1-3], (b) backward wave oscillation [2-4], and (c) absolute instability [5,6] near the band edges, at which the group velocity is zero. Among the three types, (c) is least studied. This paper focuses on (c).

Oscillations of the regenerative type, (a), occur when there is a mismatch at the input, sever, and/or output ends of the amplifier. The partial reflections at the ends would lead to regenerative oscillation if the ‘round-trip’ gain between the two points of reflection exceeds unity. In the second type, (b), the beam directly excites a backward wave of the circuit, whose group velocity is opposite to the beam mode. This leads to backward wave oscillations even if the amplifier is well matched at both ends. In (c), the feedback is also provided internally, but the instability is a result of the beam interaction with a dispersive medium (which is not unstable itself). The oscillations occur at a frequency where the group velocity is close to zero; the forward wave and the backward wave of the circuit modes are tightly coupled. We call these zero group velocity points the ‘band edge’. Oscillations of type (c) are difficult to detect directly in experiments [7], and difficult to analyze theoretically because they usually require an intricate analysis using the Briggs-Bers criterion [5,6]. Since TWT input and output ports typically provide poor matches near the band edge frequencies, oscillations of type (c) could also be masked by oscillations of type (a), occurring in the same range of frequency.

The motivation for the present work arises from our study of random manufacturing errors on TWT’s. The multiple, small-scale internal reflections due to manufacturing errors that are randomly distributed along the TWT axis may lead to large gain ripples in the frequency response [8]. It is natural to inquire if these gain ripples, due to internal reflections, may develop into an absolute instability in a TWT [9].

Band-edge oscillations in TWT’s have been intensively studied [2-4,10-18] and threshold conditions have been obtained in many cases. However, the question of whether the resulting instability is convective or absolute has received relatively little attention in the West. This important question, however, was extensively analyzed in the former Soviet Union [15,18]. These prior works adopted two simplifying assumptions: that the beam-circuit interaction is weak, and that the circuit dispersion relation near the band edge is approximated by a parabola.

Our present paper relaxes these assumptions in a case study, but corroborates other results of these earlier works.

Since the Briggs-Bers criterion requires consideration of the dispersion relation in the entire lower half complex ω -plane (in a small signal theory with $e^{j\omega t - jkz}$ dependence), we shall consider a dielectric TWT for which the exact dispersion relation can be derived. No assumption on weak beam-circuit interaction or on circuit mode is made as in previous studies [9,15,18]. The model consists of a sheet electron beam of surface charge density σ_0 , propagating in the mid-plane of a smooth dielectric, planar transmission line at speed v and guided by an infinite magnetic field, both in the z -direction. Despite its impracticality, this dielectric TWT is governed by the *exact* dispersion relation [19],

$$F(\omega, k) = \omega_p^2, \quad F(\omega, k) \equiv -(\omega - kv)^2 / [(pa) \tan(pa)]. \quad (1a,b)$$

In Eq. (1), $p^2 = \omega^2 \epsilon \mu_0 - k^2$, $\omega_p^2 = |e\sigma_0| / 2m\epsilon a$, where ϵ is the dielectric constant of the planar transmission line of separation $2a$, and μ_0 is the free space permeability. (We pretend that this dielectric medium is transparent to beam propagation.) The cold tube dispersion relation is shown in Fig. 1, given by $F(\omega, k) = 0$, or $pa = (n - 1/2)\pi$, where $n = 1, 2, 3, \dots$ and the cutoff frequency of the n -th mode is $\omega_{cn} = (n - 1/2)\pi c_\epsilon / a$ with $c_\epsilon = 1/\sqrt{\epsilon \mu_0}$. Applying the Briggs-Bers criterion [5,6] to the exact dispersion relation (1), we find the surprising result that there is no absolute instability in this dielectric TWT, regardless of the beam current, or ω_p^2 . Note that the exact dispersion relation, Eq. (1), relaxes the assumption of weak coupling. In the next two paragraphs, we present some details of the Briggs-Bers criterion for the dielectric TWT because they are relevant to the subsequent studies of both upper and lower band edges.

An absolute instability with unstable mode frequency ω_s with $\text{Im}(\omega_s) < 0$, and wave number k_s may occur when the beam current, measured by ω_p^2 in Eq. (1), is sufficiently high. It is anticipated that ω_s is close to the cutoff frequency ω_{c1} , because the reverse propagating waveguide mode needs to be internally excited for the existence of absolute instability. The complex numbers, ω_s and k_s , are determined by solving the two equations [5,6],

$$F(\omega_s, k_s) = \omega_p^2, \quad \left. \frac{\partial F(\omega, k)}{\partial k} \right|_{\omega_s, k_s} = 0. \quad (2a,b)$$

At marginal stability, ω_s is real, and this will occur at a threshold value of ω_p . If at a higher value of ω_p for which $\text{Im}(\omega_s) < 0$, an absolute instability exists. An additional test for ω_s being the root of potential absolute instability is to allow ω to change continuously from ω_s to $\omega_s - j\infty$ [5,6]. If an absolute instability exists, the (double or multiple) roots of k obtained by solving $F(\omega, k) = \omega_p^2$ would change continuously from the (double or multiple) root k_s to roots of k that end up with both $\text{Im}(k) > 0$ and $\text{Im}(k) < 0$. Such a root of ω_s and k_s is also known as the ‘pole-pinch’ root. If all of the (double or multiple) root k_s end up with the same sign in $\text{Im}(k)$ as $\omega \rightarrow \omega_s - j\infty$, there is no absolute instability and the amplifier is zero-drive stable, i.e., the amplifier is stable in the absence of an input (drive) signal. The black lines in Fig. 2 show the marginal stability curves, the k_s vs ω_s plots for real ω_s that satisfies Eq. (2b) and the pole-pinch condition. The points P_1 and P_2 correspond to $(\omega_s, k_s) = (\omega_{s1}, 0)$, and $(\omega_{s2}, 0)$, respectively, i.e. P_1 and P_2 are the first and second cutoff frequency points; Q_1 is the presumed operating point of this dielectric TWT. Since Eq. (1a) gives $\omega_p^2 = F(\omega_s, k_s)$, we have separated in Fig. 2 the values of (ω_s, k_s) at which $F(\omega_s, k_s)$ is real and non-negative. The marginal stability curves in the colored region of Fig. 2 satisfy this requirement. On the marginal stability curves in the white region, $F(\omega_s, k_s)$ is real but negative, which are unacceptable because they correspond to a negative value of ω_p^2 (but are quite relevant to the analysis of the upper band edge of a coupled cavity TWT, and to the gyrotron TWT, as we shall see below).

Since $F(\omega_s, k_s) = 0$ at the cutoff frequencies P_1 and P_2 in Fig. 2, this creates the (false) impression that there is no threshold current for the onset of absolute instability since the value of ω_p^2 is zero at marginal stability. Exactly the opposite is true, namely, there *is no absolute instability regardless of the beam current (or ω_p^2)*, in the sense of Briggs and Bers. The reason follows. As we increase ω_p^2 from zero, the pole pinch root (ω_s, k_s) remains real and it simply moves from P_1 along the marginal stability curve into the colored region of Fig. 2. This is true

for all positive values of ω_p^2 . Thus, there is no absolute instability for the dielectric waveguide TWT, as modeled by the dispersion relation, Eq. (1). While Fig. 2 assumes $v = 1.2 c_\epsilon$, we expect this conclusion to hold independent of the beam voltage. Note that on the lower boundary of the colored region that includes P_1 (Fig. 2), $F(\omega, k) = 0$. On the upper boundary of that colored region, $F(\omega, k) \rightarrow \infty$. Figure 2 shows that the value of $\bar{\theta}$, which is related to $F(\omega, k)$ by $F(\omega, k)a^2 / c_\epsilon^2 = 2 \tan(\pi\bar{\theta})$. Thus, $F(\omega, k)$ increases from zero at P_1 to infinity along the marginal stability curve in the colored region.

To further explore this lack of absolute instability, we approximate Eq. (1) with the “standard” form near operating point Q_1 (Fig. 1),

$$(\omega - kv)^2 (\omega^2 - k^2 c_\epsilon^2 - \omega_{c1}^2) = 2\omega_{c1}^4 C^3. \quad (3)$$

In Eq. (3), the first parenthesis represents the beam mode, the second parenthesis represents the $n = 1$ circuit mode, and the interaction between the two modes is represented by the RHS of (3), in which C^3 is proportional to the beam current (or ω_p^2). In Eq. (3), C is Pierce’s gain parameter [1] for the dielectric TWT. Upon applying the Briggs-Bers criterion to Eq. (3), we confirm that the dispersion relation (3) does not admit an absolute instability, regardless of the coupling constant, C^3 . The marginal stability curve in the ω - k plane for Eq. (3) is very close to the marginal stability curve in Fig. 2 in the vicinity of P_1 .

Based on the excellent approximation of Eq. (1) by the much simpler and physically transparent form of Eq. (3), we postulate that absolute instability near the zero group velocity point may be similarly analyzed by approximating the local dispersion relation in the form of the second parenthesis in Eq. (3). Under this assumption, it immediately follows that if the dispersion curve of the circuit mode is concave locally at the zero group velocity point (as at the lower band edge of the dielectric waveguide TWT), its interaction with the beam mode would not produce an absolute instability, for values of beam voltage that the beam line intersects the circuit mode on the “forward wave” side. The same conclusion was reached by Kuznetsov et al. [15,18] who approximated the vacuum circuit mode as a parabola in the ω - k plane, instead of a hyperbola that is modeled by the second parenthesis of Eq. (3). This is the case even if in the dispersion relation (3) is modified by replacing ω with $\omega - \omega'$ and k by $k - k'$ where ω' and k'

are arbitrary real constants (pretending the RHS of (3) is a constant, independent of ω and k). Shifting ω by ω' and k by k' would simply shift the coordinates of the ω - k plane, leaving the structure of the dispersion relation (3), and its analysis by the Briggs-Bers criterion unchanged.

For a coupled cavity or folded waveguide TWT, the dispersion diagram for the circuit mode [2,3], and for the beam mode is shown in Fig. 3a. The circuit mode has a zero group velocity point at the lower band-edge (A) and at the upper band-edge (B), with midband frequency at Q (Fig. 3a). Near Q, the Pierce dispersion relation reads,

$$(\omega - kv)^2[(\omega - \omega_0) - v_g(k - k_0)] = \omega_0^3 C^3, \quad (4)$$

where v_g is the group velocity of the (forward) circuit wave at the operating point Q at which $\omega = \omega_0$ and $k = k_0$, with Pierce gain parameter C . When we use the more complete dispersion relation, similar to Eq. (3), that is also valid at the lower band edge (A), it is immediately clear that the lower band-edge (A) would not be subjected to absolute instability because the dispersion curve at A is concave, and the interaction with the beam mode there is entirely analogous to that in the dielectric TWT shown in Fig. 1.

To examine the upper band-edge, B (Fig. 3a), we include the reverse propagating mode there and modify Eq. (4) to read,

$$(\omega - kv)^2[(\omega - \omega_m)^2 - r^2(k - k_m)^2 - \Delta^2] = -2\omega_0^4 C^3. \quad (5)$$

In Eq. (5), the square bracket represents the circuit mode near the upper band-edge B, and ω_m , k_m , r , and Δ are real constants, determined by the curvature at B, and by the requirement that the dispersion relation (5) reduces to the third degree polynomial, Eq. (4), near the operating point Q. In sharp contrast to Eq. (3), the RHS of Eq. (5) contains a negative sign. Thus, at the upper-band edge, the behavior of the dispersion relation, Eq. (5), is entirely analogous to that shown in Eq. (3) in which C^3 replaced by $-C^3$, i.e., ω_p^2 in Eq. (1) is replaced with $-\omega_p^2$. In the marginal stability analysis for the upper band-edge, we then would have to examine the trajectory of the marginal stability curve into the uncolored region, from the Point P₁ in Fig. 2. On the portion of the marginal stability curve that is in the uncolored region, $F(\omega_s, k_s)$ is negative and we find that there is a maximum value of $|F(\omega_s, k_s)|$. This means that at the upper band-edge, there will

be an absolute instability if the beam current is so high that ω_p^2 exceeds this maximum value of $|F(\omega_s, k_s)|$. A similar conclusion concerning absolute instability at the upper band edge was also reached if the vacuum circuit mode is approximated as a parabola in the ω - k plane, as in Refs. [15, 18] and [9].

Because of the negative sign in its RHS, the dispersion relation, Eq. (5), has the same form as that of a gyro-TWT [7,20] whose power gain originates from a “negative mass” effect [21] (also known as the cyclotron maser effect [22]). Because of this negative mass effect, C^3 is in fact negative when the gyro-TWT dispersion relation is cast in Pierce’s form [7,20,23,24]. The dispersion relation (5) then has a mathematical structure that is identical to the gyro-TWT which exhibits absolute instability [7,22]. We have applied the Briggs-Bers criterion to the dispersion relation, Eq. (5), to numerically obtain the threshold of C^3 for the onset of absolute instability at the upper band-edge of a coupled cavity TWT. We find these threshold values to be consistent with those given analytically for gyro-TWT [7].

Figure 3b shows the circuit mode, beam mode, and the marginal stability curve for the onset of absolute instability at the upper band edge for a model of the coupled cavity TWT [25]. The parameters in Eq. (5) for this example are: upper band edge frequency $\omega_u/2\pi = 36.954$ GHz, lower band edge frequency $\omega_l/2\pi = 24.245$ GHz, $\omega_m/2\pi = 44.319$ GHz, $k_m = 2\pi/L$, $r = 8.6973 \times 10^7$ m/s, $\Delta/2\pi = 7.365$ GHz, and $L = 1.765$ mm. For a beam voltage of 14.811 kV, for which $\omega_0/2\pi = 31.689$ GHz, $k_0 = 1.584\pi/L$, the threshold value of C is 0.0248 (Fig. 3b). If $C > 0.0248$, absolute instability near the upper band edge occurs. Figure 4 shows the threshold value of C at other beam voltages. The beam mode with beam voltage of 12.545 kV would intersect the circuit mode at the upper band-edge B (Fig. 3b) for which the threshold value of C is zero (Fig. 4).

If the absolute instability occurs very close to cutoff, it may easily escape detection because of the zero group velocity. For example, in the gyro-TWT, the absolute instability very close to waveguide cutoff was predicted [7], and was actually recorded in experiments but was not noted, because the power from the absolute instability that was coupled out (at the cutoff frequency) was much smaller than that due to reflection (at the operating frequency) [7,22]. Likewise, for the linear beam tube, at both lower and upper band-edge, matching is difficult,

oscillation of the reflective type would make the absolute instability of the type under discussion difficult to detect. Absolute instability at the upper band-edge may provide an intrinsic limitation of TWT efficiency. As the electron beam yields its kinetic energy to the RF, the slope of the beam line in Fig. 3a will gradually decrease, and if the beam line cuts the circuit dispersion diagram at B, oscillation due to absolute instability could occur. At Point B, the threshold current for the onset of absolute instability is zero according to the dispersion relation Eq. (5). In fact, such “drive induced” oscillation has been well documented in TWT’s [18, 26-31]. This oscillation occurs only at a high drive level – which induces significant beam velocity/energy spreads at the same time reducing the slope of the beam mode (Fig. 3a). This would lead to intersection of the (modified) beam mode with the circuit mode at point B more likely. Whether drive induced oscillation in coupled cavity TWT is related to absolute instability remains to be examined.

The absence of absolute instability at the lower band-edge (A) does not rule out an instability whose amplitude exponentiates as $\exp(\alpha t^\beta)$ for some positive α, β with $0 < \beta < 1$. Such exponential growth, in fractional power of t , is not covered by the Briggs-Bers criterion [5,6], but is common in beam breakup instability found in all types of linear accelerators, from induction linacs to linear colliders [32]. In the latter case, communication between adjacent cavities is achieved only by the beam, e.g., by setting the term $k^2 c_e^2 = 0$ in Eq. (3). [32, 33]

In summary, we find that there is no absolute instability in an exact dielectric TWT model, regardless of the beam current. We contrast the absolute instability in a gyrotron-TWT and in a linear beam TWT. Approximating the dispersion diagram as a hyperbola near the band edges, we also find that a linear beam would not excite an absolute instability close to a zero group velocity point if the dispersion diagram is concave at that point, for values of beam voltage such that the beam line intersects the circuit mode on the forward wave side. An absolute instability will occur if the dispersion diagram is convex at that point if the beam current exceeds a certain threshold value, (or if the beam line intersects the backward wave side of the circuit dispersion curve). These general conclusions are applicable to novel TWT’s of current interest, including meta-materials TWT [34,35,36], and the THz Smith-Purcell radiation sources [37,38,39]. Recent simulations indeed reveal an absolute instability at the upper band edge of a TWT that uses a disk-on-rod slow wave structure [40].

This work was supported by AFOSR Grant Nos. FA9550-09-1-0662 and FA9550-14-1-0309, and by L-3 Communications Electron Device Division.

References

1. J. R. Pierce, *Traveling Wave Tubes*, Van Nostrand (New York, 1950).
2. J. F. Gittins, *Power Travelling Wave Tubes*, Elsevier (New York, 1965).
3. A. S. Gilmour, *Microwave Tubes*, Artech House (Norwood, MA, 1986).
4. H. R. Johnson, *Proc. IRE.* **43**, 684 (1955).
5. R. J. Briggs, *Electron Stream Interactions with Plasmas*, MIT Press (Cambridge, MA, 1964).
6. A. Bers, *Handbook of Plasma Physics*, M. N. Rosenbluth and R. Z. Sagdeev, Eds., North-Holland (New York, 1983).
7. Y. Y. Lau, *et al.*, *Int. J. Infrared Millimeter Waves.* **2**, 373 (1981).
8. D. Chernin, *et al.*, *IEEE Trans. Electron Devices* **59**, 1542 (2012).
9. L. K. Ang and Y. Y. Lau, *Phys. Plasmas* **5**, 4408 (1998).
10. J.A. Reutz, in 4th International Congress on Microwave Tubes, Eindhoven, Netherlands, pp. 94-98 (1962).
11. R. W. Gould, *IRE Trans. Elect. Dev.*, **ED-5**, 186-195 (1958).
12. D.G. Dow, *IRE Trans. Elect. Dev.*, **ED-7** 123-131 (1960).
13. R.M. Bevensee, *J. Electronics and Control*, **9** 401-437 (1960).
14. A.J. Bahr, *IEEE Trans. Electr. Dev.* **ED-12** 547-556 (1965); S. O. Wallander, *IEEE Trans. Electr. Dev.* **ED-19** 655-660 (1972).
15. A. P. Kuznetsov and S. P. Kuznetsov, *Sov. Radiophys. Electron.*, **27**, 1575–1583 (1984); *Izv. Vyssh.Uchebn. Zaved., Radiofizika* **23**, 1104 (1980); N. O. Bessudnova and A. G. Rozhnev, *Tech. Phys. Lett.* **26**, 418 (2000).
16. S. M. Miller, *et al.*, *Phys. Plasmas* **1** 730–740 (1994).
17. T.M. Antonsen, *et.al.*, *IEEE Trans. Plasma Sci.*, **30** 1089-1107 (2002).
18. A.P. Kuznetsov, *et.al.*, *Radiophysics and Quantum Electronics* **47** 356-373 (2004) .

19. I. M. Rittersdorf, PhD dissertation, University of Michigan, Ann Arbor (2014); Y. Y. Lau and D. Chernin, *Phys. Fluids* **B4**, 3473 (1992).
20. K. R. Chu, *et al.*, *IEEE Trans. Microwave Theory and Techniques* **28**, 313 (1980).
21. Y. Y. Lau, *IEEE Trans. Electron Devices* **29**, 320 (1982).
22. K. R. Chu, *Rev. Mod. Phys.* **76**, 489 (2004); K. R. Chu, *et al.*, *Phys. Rev. Lett.* **74**, 1103 (1995).
23. G. Dohler and D. Gallagher, *IEEE Trans. Electron Devices* **35**, 1730 (1988).
24. Richard G. Carter (private communication) recently also noted the negative sign in front of C^3 when the gyrotron TWT dispersion relation is cast in the form of Pierce.
25. B. Levush *et al.*, in *IEEE Int'l Vacuum Electronics Conference*, Paris (2013).
26. G. Busacca, V. Meli, and M. Spalla, in *16th European Microwave Conference*, pp.174-179 (1986).
27. W.R. Ayers and Y. Zambre, in *Int'l Electron Devices Meeting (IEDM)*, pp. 957-960 (1992).
28. I. Tammaru, *Physica Scripta* **T71**, 50-59 (1997).
29. A.N. Vlasov, *et al.*, in *IEEE Int'l Vacuum Electronics Conference*, pp. 75-76 (2014).
30. R. Begum and J. Ramirez-Aldana, in *IEEE Int'l Vacuum Electronics Conference*, pp. 77-78 (2014).
31. M. Cusick, *et al.*, in *IEEE Int'l Vacuum Electronics Conference*, pp. 225-226 (2012).
32. Y. Y. Lau, *Phys. Rev. Lett.* **63**, 1141 (1989).
33. W. K. H. Panofsky and M. Bander, *Rev. Sci. Instrum.* **39**, 206 (1968).
34. D. Shiffler *et al.*, *IEEE Trans. Plasma Sci.* **38**, 1462 (2010); D. French *et al.*, *Phys. Plasmas* **20**, 8 (2013).
35. Y. S. Tan and R. Seviour, *Europhysics Lett*, **87**, 34005 (2009).

- 36. S. Liu *et al.*, *Appl. Phys. Lett.* **104**, 201104 (2014).
- 37. J. H. Booske, *Phys. Plasmas* **15**, 055502 (2008).
- 38. J. H. Booske, *et al.*, *IEEE Trans. Terahertz Sci. Technol.*, **1**, 54 (2011).
- 39. P. Zhang, L. K. Ang, and A. Gover, *Phys. Rev. ST Accel. Beams* **18**, 020702 (2015).
- 40. B. Hoff, P. Wong, and D. H. Simon, private communication.

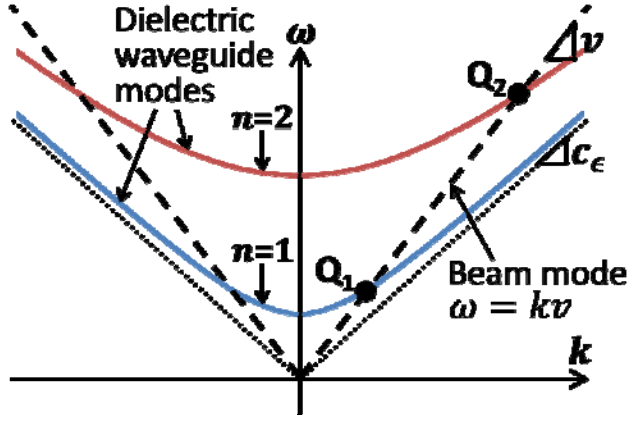


Fig. 1. (Color online) The first two waveguide modes ($n = 1$ and $n = 2$) and the beam mode in a dielectric TWT, with possible operating points at Q_1 and Q_2 .

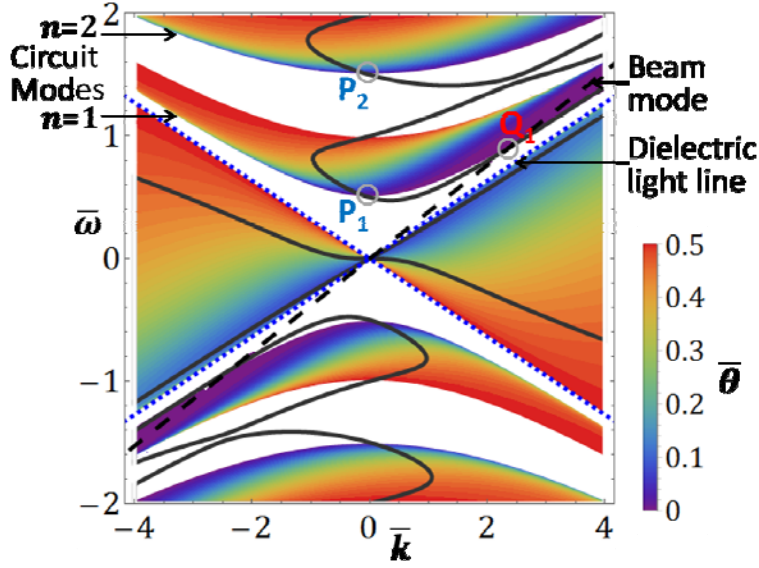


Fig. 2. (Color online) The black lines show the marginal stability curves for a dielectric TWT in the normalized ω - k plane where $\bar{\omega} = \omega a / \pi c_\epsilon$, $\bar{k} = ka$. In the colored region, $F(\omega, k) > 0$. In the non-colored region, $F(\omega, k) < 0$. The color bar shows the value of $\bar{\theta}$ in the colored regions, which is related to $F(\omega, k)$ by $F(\omega, k)a^2 / c_\epsilon^2 = 2 \tan(\pi \bar{\theta})$. On the lower (upper) boundary of the colored region that includes the cutoff frequency point P_1 , $F(\omega, k) = 0$ (= infinity).

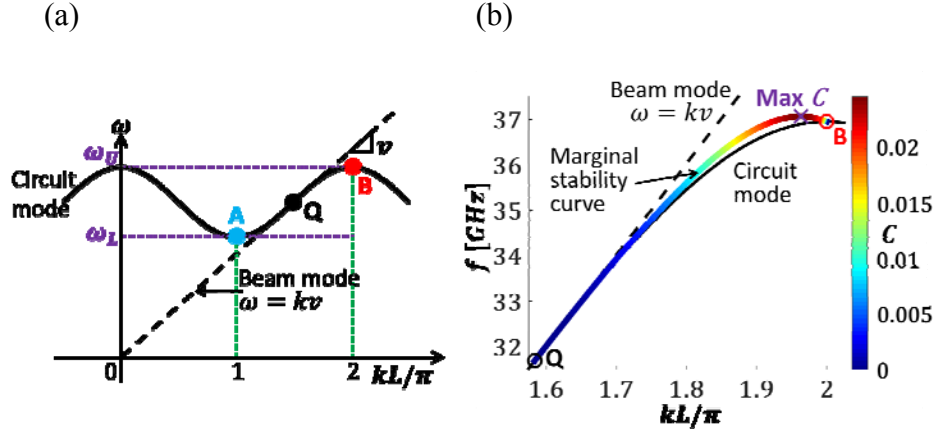


Fig. 3. (Color online) (a) Left. The lower band-edge (A), the upper band-edge (B), and the operating point (Q) at which the beam mode intersects with the circuit mode in a coupled cavity TWT at $(\omega, k) = (\omega_0, k_0)$. kL is the phase shift per period. (b) Right. The beam mode, the circuit mode, and the marginal stability curve for a Ka-band coupled-cavity TWT with a 14.811 kV beam. The maximum value of C is 0.0284 on the marginal stability curve, on which the value of C is color-coded.

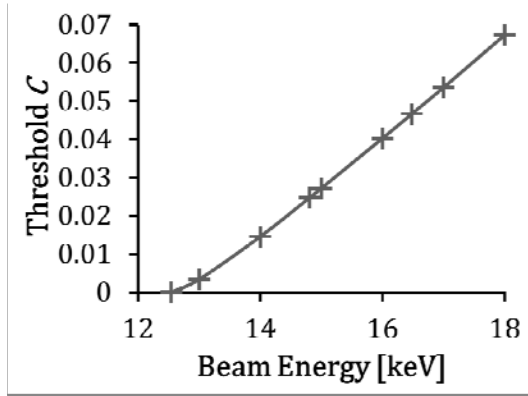


Fig. 4. Threshold value of Pierce gain parameter C for the onset of absolute instability at the upper band-edge of the coupled cavity TWT model shown in Fig. 3b.